11-20-2017

An X-Ray Study of Two B+B Binaries: AH Cep and CW Cep

Richard Ignace
East Tennessee State University, ignace@etsu.edu

K. T. Hole
Norich University

Lidia M. Oskinova
University of Postdam

J. P. Rotter
Norwich University

Citation Information

Ignace, Richard; Hole, K. T.; Oskinova, Lidia M.; and Rotter, J. P.. 2017. An X-Ray Study of Two B+B Binaries: AH Cep and CW Cep. *Astrophysical Journal*. Vol.850(1). 82. https://doi.org/10.3847/1538-4357/aa93ea ISSN: 0004-637X

An X-Ray Study of Two B+B Binaries: AH Cep and CW Cep

The Astrophysical Journal, 850:82 (7pp), 2017 November 20 https://doi.org/10.3847/1538-4357/aa93ea

An X-Ray Study of Two B+B Binaries: AH Cep and CW Cep

R. Ignace[1], K. T. Hole[2], L. M. Oskinova[3,4], and J. P. Rotter[2]
[1] Department of Physics and Astronomy, East Tennessee State University, Johnson City, TN 37663, USA; ignace@etsu.edu
[2] Department of Physics, Norwich University, Northfield, VT 05663, USA
[3] Institute for Physics and Astronomy, University Potsdam, D-14476 Potsdam, Germany
[4] 4 Kazan Federal University, Kremlevskaya Str., 18, Kazan, Russia
Received 2017 May 30; revised 2017 October 11; accepted 2017 October 12; published 2017 November 20

Abstract

AH Cep and CW Cep are both early B-type binaries with short orbital periods of 1.8 days and 2.7 days, respectively. All four components are B0.5V types. The binaries are also double-lined spectroscopic and eclipsing. Consequently, solutions for orbital and stellar parameters make the pair of binaries ideal targets for a study of the colliding winds between two B stars. *Chandra* ACIS-I observations were obtained to determine X-ray luminosities. AH Cep was detected with an unabsorbed X-ray luminosity at a 90% confidence interval of $(9\text{–}33) \times 10^{30}$ erg s^{-1}, or $(0.5\text{–}1.7) \times 10^{-7} L_{\rm Bol}$, relative to the combined Bolometric luminosities of the two components. While formally consistent with expectations for embedded wind shocks, or binary wind collision, the near-twin system of CW Cep was a surprising nondetection. For CW Cep, an upper limit was determined with $L_X/L_{\rm Bol} < 10^{-8}$, again for the combined components. One difference between these two systems is that AH Cep is part of a multiple system. The X-rays from AH Cep may not arise from standard wind shocks nor wind collision, but perhaps instead from magnetism in any one of the four components of the system. The possibility could be tested by searching for cyclic X-ray variability in AH Cep on the short orbital period of the inner B stars.

Key words: stars: early-type – stars: individual (AH Cep, CW Cep) – stars: massive – stars: winds, outflows – X-rays: binaries

1. Introduction

The modern era has brought forth a plethora of intriguing results for the study of massive stars based on X-ray observations (e.g., Oskinova 2016). Massive star binaries with colliding winds (colliding wind binaries, hereafter "CWBs") have been a staple of X-ray studies, both theoretically and observationally (e.g., Usov 1992; Stevens et al. 1992; Rauw & Nazé 2016). The attractions for stellar astronomers have been the prospects of luminous and hard X-ray emissions from CWBs, combined with possibilities for inferring or constraining wind properties (such as mass-loss rates $\dot{M}$), orbital properties, and interesting plasma physics (instabilities, possibly magnetism, or nonequilibrium effects).

Advances in the modern era have been driven by increases in the numbers of objects that have been studied via surveys (e.g., Nazé et al. 2011), plus intensive studies of a limited number of especially interesting targets (some recent examples include Lomax et al. 2015; Gosset & Nazé 2016; Corcoran et al. 2017). One omission to the effort has been the neglect of CWBs consisting of B+B stars. Much of the previous focus on CWBs has involved systems in which one component is a Wolf–Rayet (WR) star. The reason is clear: WR stars have fast winds and generally large mass-loss rates that can result in strong X-ray emissions (Cherepashchuk 1976; Prilutskii & Usov 1976). With modern X-ray telescopes, interest has also been shown in what are usually X-ray fainter O+O binaries (e.g., Pittard & Parkin 2010; Rauw et al. 2016). Owing to low mass-loss rates, B+B binaries have not, to our knowledge, been modeled in hydrodynamic simulations, nor the subject of a dedicated observational study.

Yakut et al. (2007) reported on a study of the B+B binary CV Vel. In that paper, the authors summarized the properties for 17 fairly short-period and mostly main-sequence B+B binaries. What makes this list special is that all of the systems are both double-lined spectroscopic and eclipsing systems with relatively short orbital periods. Analyses from a variety of authors have provided for well-constrained orbital and stellar parameters of these systems, including masses, radii, temperatures, luminosities, semimajor axes, and eccentrities, among other things. In particular, the viewing inclinations are known to be near edge-on.

As a result, we selected the two most massive binaries of the listing—AH Cep and CW Cep—with the intent of detecting evidence for a wind–wind collision between B stars using the *Chandra* X-ray Telescope. This paper describes expectations for the observations, and reports on the curious result of one detection and one nondetection, despite the two systems being near twins in their physical parameters. Section 2 describes target selection and predicted X-ray levels. Section 3 details the observations. Results from the pointings are discussed in relation to these expectations in Section 4, with concluding remarks offered in Section 5.

2. Predicted X-Ray Emissions for CWBs

2.1. Target Selection

Table 8 of Yakut et al. (2007) lists 17 B+B binaries along with primarily stellar properties of the components, plus the orbital period ($P_{\rm orb}$). All but one of the binaries have orbital periods under 1 week. The binary pairs usually consist of the same spectral type, from B0.5V+B0.5V to B9.5V+B9.5V, although a few systems consist of pairs with different spectral-type components (one is B9V+A0V).

The two most massive binaries are comprised of B0.5 V stars: AH Cep (B0.5Vn+B0.5Vn) and CW Cep (B0.5V +B0.5V). Table 1 summarizes the stellar properties of these systems; Table 2 summarizes their orbital properties. We adopt the standard usage that the primary is the more massive star,

Table 1
Stellar Parameters

	AH Cep (primary)	AH Cep (secondary)	CW Cep (primary)	CW Cep (secondary)
Sp. Type	B0.5n	B0.5n	B0.5	B0.5
$T_{\rm eff}$ (K)	30,000	29,000	28,000	28,000
Mass ($M_\odot$)	15.4	13.6	13.5	12.1
Radius ($R_\odot$)	6.4	5.9	5.7	5.2
Luminosity ($10^4\,L_\odot$)	2.9	2.1	1.9	1.4
$v_{\rm esc}$ (km s^{-1})	960	940	950	940
v_∞[a] (km s^{-1})	1400	1400	1400	1400
$\dot{M}$[a] ($10^{-9}\,M_\odot$ yr^{-1})	2.5	2.2	1.8	1.8

Note.
[a] The wind terminal speeds and mass-loss rates are not measured properties, but estimated ones. See Section 2.

Table 2
Orbital Parameters

	AH Cep	CW Cep
$P_{\rm orb}$ (day)	1.78	2.73
a ($R_\odot$)	19.0	24.2
e	0.0	0.0
$q = M_2/M_1$	0.88	0.90

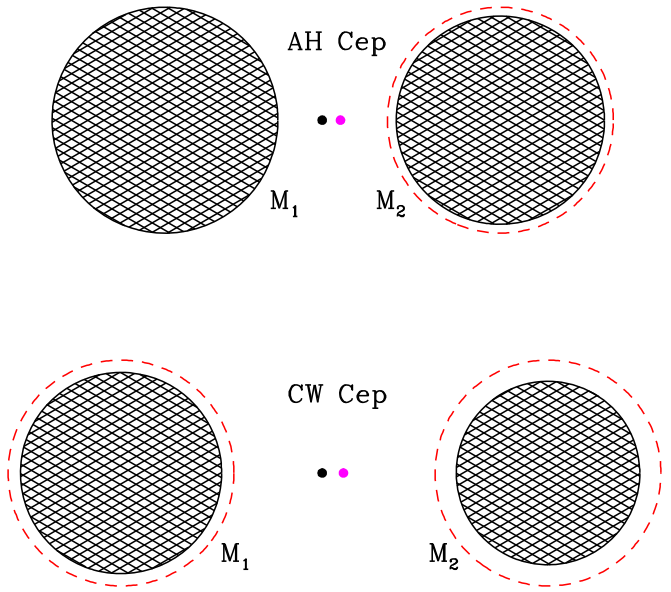

Figure 1. Scale representation of the two binary systems. Upper is AH Cep; lower shows CW Cep. Primary and secondary stars are indicated by the labels M_1 and M_2, respectively. The dashed red circles represent the size of the primary for AH Cep, as a reference guide. The solid black dot is the center of mass. The stars are situated in the figure such that the center of mass is at the origin of the coordinate system for each binary. The magenta dot signifies our estimate for the location of the colliding wind stagnation point (see Section 2).

and the secondary is the less massive star, signified with subscripts "1" for primary and "2" for secondary. Note that the mass-loss rates and terminal speeds are not measured but calculated from models. This will be discussed further in Section 2.2.

Although all four stars in these two binaries share the same spectral type (aside from the peculiar designation "n"), the stellar properties are not exactly identical. Both binaries have mass ratios $q = M_2/M_1$ of about 0.9. The masses range from 12 to 15 $M_\odot$. The luminosities range by a factor of 2 from the least luminous (secondary for CW Cep) to the most luminous (primary for AH Cep). Regarding the orbits, both binaries have orbital periods of ∼2 days, and the orbits are circular (Kim et al. 2005; Yakut et al. 2007, for AH Cep and CW Cep, resp.).

Figure 1 provides a schematic for the relative sizes and separations of the stars. The two systems are displayed on the same scale and offset vertically from one another. Between the stars, the black dot indicates the location of the center of mass (CM). The figure is arranged so that the respective CM points are the coordinate origins for the two systems. Nearby in magenta are the respective stagnation points, as discussed further in Section 2.2. The primary for AH Cep is the largest of the four stars, and its size is shown as a red dashed circle around the other three stars for reference.

Ultimately, major considerations for the selection of AH Cep and CW Cep included the following.

1. The two binaries are the most massive ones in the list of Yakut et al. (2007), suggesting that they will be the most X-ray luminous, even without detection of a colliding wind interaction (hereafter, CWI), based on the scaling that $L_X \sim 10^{-7}\,L_{\rm Bol}$ for massive, single stars (e.g., Berghoefer et al. 1997; Nazé 2009).
2. For each binary, the component stars are nearly identical. This suggests that the winds will be nearly identical as well, and so the CWI will be located close to the CM for each of the respective systems. This should simplify the intrepretation of any detected emissions from the CWIs.
3. Given that the stars are so similar in mass, size, and binary orbit (inclination and period), observed differences in X-rays could more confidently be related to "secondary" considerations, such as stellar magnetism.

2.2. Expected X-Ray Properties

The driving goal for obtaining *Chandra* data for AH Cep and CW Cep is to detect for the first time a "classical" wind collision (i.e., not involving magnetospheric effects) among B +B binaries. Failing in that, we expected to detect X-ray emissions at the level predicted for single massive stars.

For X-ray emissions from the individual stellar winds, we had anticipated that, being of quite early types in the B spectral class at B0.5, the individual stars would follow the relation of $L_X \sim 10^{-7}\,L_{\rm Bol}$ (see Oskinova 2016 and references therein). Table 3 provides estimates for the X-ray luminosities L_{X*}, with subscript "$*$" referring to the stellar components of the binaries. These values are totals for the two components, treating each one as adhering to the relation for single stars. This canonical scaling for single stars is known to have significant dispersion, and its extension much into the B spectral class is recognized as dubious (e.g., Cohen et al. 1997; Nazé 2009; Owocki et al. 2013).

For X-rays from a colliding wind, the situation is far more speculative. First, such estimates require knowledge of the mass-loss rates $\dot{M}$ and terminal speeds v_∞ of the stellar winds.

For a rough estimate of the wind speed, we adopted a scaling from the theory of Castor et al. (1975, CAK) for line-driven winds. The first is that the wind terminal speed scales as $v_\infty \propto v_{\rm esc}$. For B stars, we adopt a value of 1.5 for the ratio, for which all four stars are estimated to have $v_\infty \approx 1400$ km s^{-1}, as indicated in Table 1.

Table 3
Predicted X-Ray Properties

	AH Cep	CW Cep
d (pc)	1020	640
$E(B-V)$	0.51	0.59
$N_{\rm H}$ (10^{21} cm^2)	3.0	3.4
$L_{X,*}$ (10^{30} erg s^{-1})	19	12
η_∞	0.83	0.85
ζ_∞	0.91	0.92
$\theta_{\rm Sh}$ (radiative)	87°	88°
$\theta_{\rm Sh}$ (adiabatic)	87°	87°
$kT_{\rm peak}$ (keV)	0.29	0.69
χ	2	20
$L_{X,\rm CWI}$ (10^{30} erg s^{-1})	>4.6[a]	>2.0[a]

Note.
[a] Values scaled from Pittard & Parkin (2010), evaluated at terminal speed. At less than terminal speed, Equation (9) indicates a larger X-ray luminosity.

For the mass-loss rates, the following relation was used from Vink et al. (2000):

$$\log \dot{M} = -22.7 + 8.96\, T({\rm kK}) - 1.42\, T^2({\rm kK}), \quad (1)$$

which is claimed to have validity for $T > 15$ kK. Here the mass-loss rate is in solar masses per year. For AH Cep and CW Cep, values for $\dot{M}$ are given in Table 1. In an analysis of *IUE* spectral data, Pachoulakis et al. (1996) set upper limits to the $\dot{M}$ values from Equation (1) for the stars in CW Cep at $1.0 \times 10^{-8}\, M_\odot$ yr^{-1} and $0.3 \times 10^{-8}\, M_\odot$ yr^{-1} for the primary and secondary components, respectively. In the case of CW Cep, the values are below the upper limits of Pachoulakis et al. (1996). Given the similarity of the stars in AH Cep to those of CW Cep, it is notable that the $\dot{M}$ values for components of AH Cep are also below the upper limits established for CW Cep.

To obtain estimates for the X-rays from colliding winds, an important parameter is the ratio of wind momentum rates for the two stars involved. This parameter is given by

$$\eta = \frac{\dot{M}_2 v_2}{\dot{M}_1 v_1}. \quad (2)$$

Note that different authors use different symbols and definitions for the ratio of wind momenta. The above follows Gayley (2009). (By contrast, Rauw & Nazé 2016 define η as the inverse of the above.) Instead of using estimated values of mass-loss rates and terminal speeds, we note that CAK theory gives $\dot{M} v_\infty \propto M_*^{3/2}$, for which case $\eta \approx q^{3/2}$, assuming that the terminal wind speeds for the components in each binary are equal. This further assumes the shock forms after the respective winds have achieved terminal speeds, which we signify as η_∞. Values of η_∞ derived in this way are listed in Table 3.

The η parameter determines the location of the stagnation point, and for an adiabatic wind, it can be used to estimate the X-ray luminosity (Stevens et al. 1992) and the opening angle of the bowshock (Gayley 2009). Let x be the fractional distance between the stars for the location of the stagnation point, from the primary. Then $1 - x$ is the fractional distance from the secondary to that point. Stevens et al. (1992) showed that

$$\zeta = \frac{1-x}{x} = \eta^{1/2}. \quad (3)$$

Consequently, for CAK theory, $\zeta_\infty \approx q^{3/4}$, again for winds at terminal speed. Values of ζ_∞ are given in Table 3. The stagnation point, using this relation, is indicated in the schematic of Figure 1 by the magenta dot.

Gayley (2009) derived the opening angle, $\theta_{\rm Sh}$ for the bowshock when the cooling is strictly adiabatic. This too relates to η via the expression $\eta = \tan^4(\theta_{\rm Sh}/2)$. Again, for CAK theory it can be shown that

$$\theta_{\rm Sh} \approx 2 \tan^{-1}\, q^{3/8}. \quad (4)$$

However, for a colliding wind shock that is radiative, Canto et al. (1996) determine the opening angle to be (using the modified version from Gayley 2009):

$$\eta = \frac{\tan\theta_{\rm Sh} - \theta_{\rm Sh}}{\tan\theta_{\rm Sh} - \theta_{\rm Sh} + \pi}. \quad (5)$$

Whether adiabatic or radiative, the derived opening angles, given in Table 3, are very close to 90°. This indicates that, neglecting the effects of the orbital motion, the discontinuity surface for the colliding winds should be nearly planar at the scale of the binary separation.

One challenge to these conclusions is the fact that the stellar components are so close to one another that the stagnation point actually lies within the wind acceleration zones of the two stars in each binary. Using a standard $\beta = 1$ wind velocity law for illustration, as often invoked for early-type winds, we have that

$$v(r) = v_\infty\left(1 - \frac{bR_*}{r}\right), \quad (6)$$

where v is the radial velocity of the spherical wind at radius r, and $b \lesssim 1$ sets the speed at the wind base. For AH Cep, the wind speed is just over a third of the terminal value at the predicted stagnation point. For CW Cep, the speeds are just over half of terminal. In both cases, the fractional speeds, v/v_∞ are almost exactly the same for the respective components, and so η is little changed. However, because the winds have not achieved terminal speed, the structure of the CWI is probably not well-represented by the scenario in which both stars have achieved terminal speed. Nonetheless, one may still expect that the shock discontinuity surface is largely planar between the stars (again, neglecting Coriolis effects that act to distort the surface from planar).

Stevens et al. (1992) provide relations for the peak temperature achieved in the wind collision, for whether the cooling is predominantly adiabatic or radiative, and if the former, a scaling relation for the X-ray luminosity. First, the peak temperature can be estimated as

$$T_{\rm peak} = 13.6\ {\rm MK}\left(\frac{v}{1000}\right)^2 = 1.17\ {\rm keV}\left(\frac{v}{1000}\right)^2, \quad (7)$$

for v in kilometers per second. Again using a $\beta = 1$ velocity law, expected peak temperatures are given in Table 3. Note that the peak value is somewhat soft at 0.3 keV in the case of AH Cep, but fairly hard at 0.7 keV for CW Cep.

Stevens et al. (1992) provide a relation for the ratio of the radiative cooling time to the flow time as a discriminant between predominantly radiative or adiabatic cooling. The ratio is

$$\chi = t_{\rm cool}/t_{\rm flow} \sim \frac{(v/1000)^4 (d/10^7)}{\dot{M}/10^{-7}}, \quad (8)$$

with v in km s^{-1}, d the instantaneous binary separation in kilometers, and $\dot{M}$ the mass-loss rate. in $M_\odot$ yr^{-1}. The value of χ is about 2 for AH Cep and 20 for CW Cep, with $\chi \gtrsim 1$ indicating that the cooling is adiabatic.

With adiabatic cooling, the X-ray luminosity is estimated with

$$L_X \propto \dot{M}^2\, v^{-3.2}\, d^{-1} (\eta^2 + \eta^{3/2}). \quad (9)$$

This expression is a proportionality. To calibrate, we use model cwb2 from Pittard & Parkin (2010) for a wind collision between identical stars of type O6 V. That model, characterized by $\chi = 19$, predicts an X-ray luminosity of $L_X = 1.6 \times 10^{33}$ erg s^{-1} in the 0.5–10 keV band. From this model, along with the above equation, X-ray luminosities can be estimated, and these are provided as expected values for the target sources in Table 3. A reminder that subscript "$*$" refers to stellar components, and "CWI" refers to contributions from the CWI. Note that the predicted values for $L_{X,\rm CWI}$ given in Table 3 are lower limits from evaluation at wind terminal speed; if the CWI forms at a lower wind speed, the expected values would be higher, based on Equation (9).[5]

3. Observations with ACIS-I

Two observations of the systems were obtained by the *Chandra* X-ray Observatory, using the Advanced CCD Imaging Spectrometer (ACIS; Garmire et al. 1992). ACIS-I was chosen for maximum sensitivity with the ability to perform some spectral analysis with a relatively short observing time. Our exposures were designed to yield similar numbers of X-ray counts, based on the discussion of the previous section. The final exposure times for the two observations were 7 ks and 10 ks for CW Cep and AH Cep, respectively. Ephemeris data from the AAVSO[6] indicates that neither system was in eclipse at the time of observation (with confirmation from Han et al. 2002 for CW Cep).

Hydrogen column densities were estimated using values of $E(B-V)$ from the relation that $N_{\rm H} \approx 5.8 \times 10^{21}$ cm^2 $\times$ $E(B-V)$ (Cox 2000). Observed colors were combined with expected ones based on spectral class using Cox (2000). Count rates for ACIS-I were then estimated with interstellar extinction included. Note that the thermal plasma of OB star X-rays is typified by temperatures of a few MK (i.e., kT values of a couple tenths of a keV (e.g., Oskinova 2016). Table 4 summarizes information about the observations, such as the exposure "Exp", observed counts, the count rate $\dot{C}$, the hardness ratio HR, and the inferred fluxes f and luminosities L with ACIS-I.

[5] Note that in the acceleration zone of the winds, peak temperature in the post-shock gas may no longer occur along the lines of center for the stars, but in an annulus about that line, owing to the condition of oblique shocks, with possible consequences for the expected X-ray luminosity. Whether this can occur requires evaluation via the hydrodynamical simulation.

[6] https://www.aavso.org/

Table 4
Measured X-Ray Properties

	AH Cep	CW Cep
R.A.[a]	22 47 52.9414	23 04 02.2185
Decl.[a]	+65 03 43.797	+63 23 48.718
Exp. (ks)	10	7
Counts	37	...
$\dot{C}$ (cps)	0.0037	<0.00033
HR	0.9	...
$f_{\rm ACIS}$[b,c] (10^{-14} erg s^{-1} cm^{-2})	7–24	<2
$L_{\rm ACIS}$[c] (10^{30} erg s^{-1})	9–33	<1.0

Notes.
[a] R.A. and decl. taken from GAIA DR1 catalog.
[b] ACIS-I fluxes are the "unabsorbed" values.
[c] ACIS-I fluxes and luminosities are for the range of 0.3–10 keV. The ranges quoted for AH Cep are 90% confidence intervals.

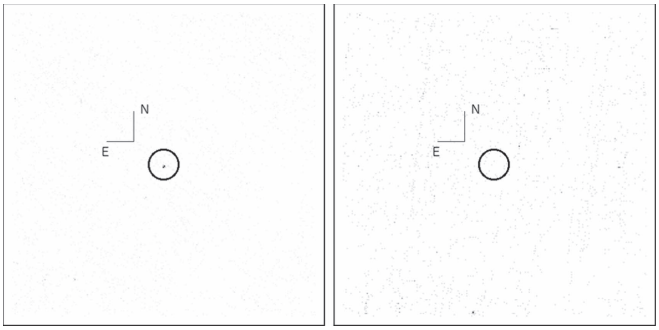

Figure 2. *Chandra* ACIS-I image of the field of view for the targets AH Cep (left; detected) and CW Cep (right; undetected). Each image is 2′ × 2′. The circles of 6″ radius are centered on source coordinates from SIMBAD.

Analysis of both observations was performed with the CIAO[7] (v4.9; Fruscione et al. 2006) software after standard pipeline processing of the event files. Source luminosity was estimated using the srcflux function, assuming an APEC model, by Dickey & Lockman (1990) via the HEASARC database[8]. Figure 2 displays the field of view for our two targets. Note that based on the GAIA DR1 Catalog, there are no other objects within 2 arcsec from either target. The overall 90% uncertainty circle of *Chandra*'s X-ray absolute position has a radius of 0.8 arcsec. The 99% limit for the positional accuracy is 1.4 arcsec. The worst case offset is 2.0 arcsec, but that is for off-axis observations, whereas both of our pointings were on-axis. For CW Cep, we detected no source photons, giving us an upper limit on the model luminosity of $\sim 1 \times 10^{30}$ erg s^{-1}. AH Cep was detected with 37 source counts, and an implied luminosity of (9–33) $\times$ 10^{30} erg s^{-1}, for a 90% confidence interval. Though the S/N is too low to be definitive, AH Cep emission does show some energy dependence, and is centered around $\approx$1 keV. We used a 1T fit with kT of 0.3 keV and 0.6 keV, typical OB star X-ray spectra, and of the expected temperature for the colliding wind shock as indicated in Table 3.

Although the detection of AH Cep yields an inferred X-ray luminosity that is basically commensurate with expectations for embedded wind shocks and/or a wind-collision shock, the

[7] Available at http://cxc.harvard.edu/ciao/.

[8] https://heasarc.gsfc.nasa.gov/cgi-bin/Tools/w3nh/w3nh.pl

nondetection of CW Cep, a near twin of the AH Cep system, makes this interpretation problematic.

4. Discussion

How are we to understand the detection for AH Cep along with the nondetection of CW Cep, given the quite similar properties of these two early-type binary stars? Uncertainties in distance and interstellar absorption could perhaps be important. However, given that one of the sources is detected and the other is not, such effects must conspire to produce an order of magnitude difference between the two source luminosities.

Alternatively, it is useful to review the assumptions of Section 2.2 for the target sources. In the theoretical study of Owocki et al. (2013) for the scaling between L_X and $L_{\rm Bol}$ for single massive stars, it seems likely that embedded wind shocks for early B-type stars, even B0.5 V stars such as our targets, will likely be adiabatic and therefore faint. In terms of the emission expected from the stars individually, we appear to have overstimated expected X-ray luminosities.

Regarding the colliding wind shock for the respective binary targets, Antokhin et al. (2004) derived a convenient expression for the condition in which the colliding wind shock is radiative or adiabatic in terms of orbital period. Their Equation (24) is reproduced here:

$$P < 26 \text{ day} \left(\frac{20\, M_\odot}{M_1 + M_2} \right)^{1/2} \frac{\dot{M}_{-6}^{1.5}}{v_{1000}^{7.5}}, \qquad (10)$$

where P is the orbital period, $\dot{M}$ is in $10^{-6}\, M_\odot$ yr^{-1}, and v is the pre-shock speed relative to 1000 km s^{-1}. The shock will be radiative when the inequality is met; otherwise, it will be adiabatic.

In the case of AH Cep, the orbital period is 1.78 days. With a terminal speed of 1400 km s^{-1}, the division between radiative and adiabatic colliding wind shocks is an orbital period of 0.001 days, or 36 s. The binary period is of course much greater, thus predicting an adiabatic shock. However, neither of the winds for the two components comes anywhere near achieving terminal speed. The orbital separation is 19.0 $R_\odot$. The primary has a radius of 6.4 $R_\odot$, and the secondary has a radius of 5.9 $R_\odot$. Again using Equation (6), the pre-shock wind speed of the primary for the distance of the stagnation point is $0.34 v_\infty$. Using $\dot{M}$ estimated for the primary only, the threshold for a radiative shock increases to 0.7 days. Although still too short for the shock to be radiative, it is much closer, being within a factor of $\sim$2.5.

Now consider CW Cep. The orbital period is longer at 2.73 days. The orbital separation is somewhat larger, and the stars are both somewhat smaller than the components of AH Cep. Following the steps in the example of AH Cep, the colliding wind shock will be adiabatic for orbital periods longer than about 0.01 days.

In summary, it appears that the embedded wind shocks for both AH Cep and CW Cep are likely adiabatic, as consistent with Equation (8), suggesting that the X-ray emissions from the individual winds, if they were in isolation, would be relatively weak. The colliding wind shocks are likewise adiabatic and weak sources. However, there is tremendous sensitivity of this criterion to the mass-loss rate and pre-shock wind speed, of which neither is well-constrained for either system. If the X-rays of AH Cep do originate from the colliding wind shock, it would imply that we have, for the first time, detected X-rays from a B+B wind collision.[9]

There is an alternative explanation to account for the detected X-rays. Several previous studies suggest that AH Cep is a multiple system, with four components in total (Mayer & Wolf 1986; Drechsel et al. 1989; Harvig 1990; Kim et al. 2005). Component #3 is assigned a period of 67.6 years in an eccentric orbit of $e = 0.52$. Component #4 has a period of 9.6 years, in an even more eccentric orbit with $e = 0.64$. The two stars have respective mass estimates of $M_3 \approx 8 M_\odot$ and $M_4 \approx 4 M_\odot$, making them spectral types B2-B3 and B7-B8, respectively (Kim et al. 2005). The age of the system is estimated at about 6 Myr (Holmgren et al. 1990). At these spectral types, neither the tertiary or quarternary stars are expected to be X-ray bright, unless perhaps the stars have magnetic fields (Oskinova et al. 2011; Petit et al. 2013; Nazé et al. 2014).

Binarity among massive stars is known to be relatively normal (e.g., a recent short review by Sana 2017). Less is known about hierarchical systems among massive stars. The well-known multiplet massive star system Mintaka (δ Ori, HD 36486) is bright, relatively close, and well-studied in many wavebands, including extensive observations at X-ray wavelengths (Corcoran et al. 2015; Nichols et al. 2015; Pablo et al. 2015; Richardson et al. 2015; Shenar et al. 2015). The center of the system is a triple, involving an O9.5 II primary and an early-type secondary in a fairly tight orbit with a period of $\approx$5.7 days. A more distant third component of perhaps $\approx 8\, M_\odot$ follows an elliptical orbit of nearly 350 years. Although Mintaka is an X-ray source, the bulk of the emission is associated with the embedded shocks for the primary wind, as opposed to a wind collision with the secondary star's wind, or as arising with the tertiary. Mintaka is a case in which the X-ray emissions are dominated by the primary star, but in contrast to our targets, the primary for Mintaka is an evolved late-type O star.

β Cru is an example of a triple system involving massive stars that displays a complex X-ray signal (Cohen et al. 2008). The primary is B0.5 III, so the same spectral class as the stars in our binaries, but a giant instead of a main-sequence star. The secondary is B2 V (Aerts et al. 1998) in an eccentric orbit with a period of 5 yr. The age of the system is estimated at around 8–10 Myr (Cohen et al. 2008), which is not much greater than the estimate for AH Cep. Interestingly, Cohen et al. (2008) report on a pre-main-sequence companion in their X-ray study of β Cru, betrayed through its relatively hard contribution to the X-ray emission detected from the system. β Cru represents a case in which the massive primary does not entirely dominate the X-ray emissions. Whereas the primary for β Cru is evolved, the primary and secondary stars in AH Cep are less luminous main-sequence stars. Consequently, either/both of the other companions could have a relatively more important contribution to observed X-ray emissions, if magnetic.

[9] Pillitteri et al. (2017) report the detection of variable X-rays from the B2IV +B2V binary ρ Oph A+B, but attribute the X-rays to magnetic effects for the fast-rotating, young primary star. Shultz et al. (2015) report on X-rays from B +B binary ϵ Lup in which both stars are magnetic with interacting magnetospheres.

5. Conclusions

There are three main mechanisms to consider for understanding the detection of X-rays from AH Cep but not from CW Cep.

1. The X-rays detected in AH Cep may come from a colliding wind shock that is either not present or not detected in CW Cep. The predictions for whether the colliding wind shock is radiative or adiabatic are quite sensitive to the velocity distribution of the stellar winds, and somewhat sensitive to the mass-loss rate. Using a $\beta = 1$ velocity law, and given the different separations between the primary and secondary stars in our targets, we may expect the colliding wind shock of CW Cep to be $\sim 3\times$ smaller than for AH Cep, yet the upper limit to the X-ray luminosity for CW Cep is over $10\times$ smaller.

   Our adopted terminal speeds may be too high, or too low. Moreover, our use of $\beta = 1$ for the velocity law could well be in error: the radiation from each of the stars may modify the wind driving in between the stars. It should be noted that Prinja (1989) provides an analysis of *IUE* spectra for a number of main-sequence B stars, among them some early types. Values for $\dot{M}$ and v_∞ are determined only for two B0 V stars, and the mass-loss rates are actually products, $\dot{M}q$, where q is the ionization fraction for the species used in the P Cygni line analysis. Consequently, the values from Prinja (1989) provide only lower limits to $\dot{M}$, which for the two B0 V stars are nearly two orders of magnitude lower than values adopted from Vink et al. (2000). The terminal speeds are also lower than what we have adopted. Using values from Prinja (1989) would indicate that the colliding wind shocks for AH Cep and CW Cep are strongly adiabatic. Although it seems unlikely that we have detected X-rays from the colliding wind shocks, the wind properties of the stars and of the CWI, being in the wind acceleration zone, are simply too poorly known.
2. It seems unlikely that we have detected wind embedded shocks from the individuals winds. The $L_X/L_{\rm Bol}$ ratio for AH Cep is low but commensurate with expectations for single stars. However, all four of the B0.5 V stars are nearly identical. Consequently, it is difficult to understand why AH Cep is detected when CW Cep is not, if the X-rays arise from wind shocks. Perhaps the primary or secondary in AH Cep is magnetic. Magnetic B stars are known to be diverse in the luminosity and hardness level of their X-rays (e.g., Oskinova et al. 2011; Petit et al. 2013; Nazé et al. 2014).
3. One distinction between our two targets is that AH Cep has been reported to be a multiplet system of four stars, whereas CW Cep appears to be only a binary. It is possible that either or both of the other two stars in AH Cep are responsible for its X-ray emissions. The tertiary and quaternary components are thought to be mid and late B stars, respectively. Detectable X-rays from embedded wind shocks for either of these objects seems highly unlikely, given the roughly $\dot{M}^2$ dependence of X-ray luminosity for these spectral types (Owocki et al. 2013). Wind collision is an equally unlikely explanation: the large separation implies low densities and small emission measures. The ratio $L_X/L_{\rm Bol}$ for the detection of the AH Cep system is $\approx 1 \times 10^{-7}$. If the B2-B3 star of the system were the source of X-rays, the ratio would increase to $\sim 10^{-6}$ for that object; if the even later B8–B9 star is the source, the ratio would be $\sim 10^{-5}$.

An interesting implication of the first two points—namely that X-rays are not detected from the stellar winds or colliding winds—would further support the emerging picture that the wind properties of B stars are poorly known, and that the winds may be quite weak. Failure to detect X-ray signatures from colliding winds could be a combination of low $\dot{M}$ values and low-speed flow. The latter would result in weaker shocks of lower temperatures at ~ 1 MK. Failure to detect X-rays from the individual winds leads to the same conclusion of weak winds. As further evidence in support of B stars having weak winds, Muijres et al. (2012) mention difficulties with obtaining wind solutions for $L \lesssim 2 \times 10^5\, L_\odot$. Their struggle aligns well with the low $\dot{M}$ and v_∞ values obtained by Oskinova et al. (2011) in their study of several magnetic B stars. The situation for the B stars is complicated by the fact that some weak-wind B stars are relatively strong X-ray emitters (Huenemoerder et al. 2012; Doyle et al. 2017).

Progress toward understanding the differences in X-ray emissions between these two systems can be addressed with new observations. Certainly, better understanding of the stellar winds would be furthered by performing a detailed analysis of UV spectra of the systems, if possible. For example, Pachoulakis et al. (1996) were only able to derive upper limits to the mass-loss rates for CW Cep. A deep X-ray exposure of CW Cep could allow for a detection of its faint X-rays, or at least place a more stringent upper limit on its emission. An X-ray light curve for the detected source, AH Cep, would constrain the source of X-rays. If its X-ray emissions vary in phase with the orbit period of the primary and secondary, then the X-rays arise from the inner binary of this multiplet. Dimming of the X-rays when either of the stars are forefront (i.e., during an optical eclipse, twice per orbit) would favor a colliding wind shock as the source of X-rays, as opposed to embedded wind shocks. Failure to detect variability of either kind could suggest stellar magnetism among any of the four components of AH Cep as an explanation for the X-ray detection.

The authors gratefully acknowledge an anonymous reviewer for making several comments that have improved this paper. Support for this work was provided by the National Aeronautics and Space Administration through *Chandra* Award Number G05-16013A issued by the *Chandra X-ray Observatory* Center, which is operated by the Smithsonian Astrophysical Observatory for and on behalf of the National Aeronautics Space Administration under contract NAS8-03060. K.T.H. and J.P.R. would like to acknowledge the Norwich University Office of Undergraduate Research and the Office of Academic Research for support of this project. The work of L.M.O. is partially supported by the Russian Government Program of Competitive Growth of Kazan Federal University. This research has made use of the SIMBAD database, operated at CDS, Strasbourg, France. We acknowledge with thanks the variable star observations from the AAVSO International Database contributed by observers worldwide and used in this research. This research has made use of data and/or software provided by the High Energy Astrophysics Science Archive Research Center (HEASARC), which is a service of the Astrophysics Science Division at NASA/GSFC and the High Energy Astrophysics Division of

the Smithsonian Astrophysical Observatory. This work has made use of data from the European Space Agency (ESA) mission *Gaia* (https://www.cosmos.esa.int/gaia), processed by the *Gaia* Data Processing and Analysis Consortium (DPAC, https://www.cosmos.esa.int/web/gaia/dpac/consortium). Funding for the DPAC has been provided by national institutions, in particular, the institutions participating in the *Gaia* Multilateral Agreement.

ORCID iDs

R. Ignace https://orcid.org/0000-0002-7204-5502

References

Aerts, C., De Cat, P., Cuypers, J., et al. 1998, A&A, 329, 137
Antokhin, I. I., Owocki, S. P., & Brown, J. C. 2004, ApJ, 611, 434
Berghoefer, T. W., Schmitt, J. H. M. M., Danner, R., & Cassinelli, J. P. 1997, A&A, 322, 167
Canto, J., Raga, A. C., & Wilkin, F. P. 1996, ApJ, 469, 729
Castor, J. I., Abbott, D. C., & Klein, R. I. 1975, ApJ, 195, 157
Cherepashchuk, A. M. 1976, SvAL, 2, 138
Cohen, D. H., Cassinelli, J. P., & MacFarlane, J. J. 1997, ApJ, 487, 867
Cohen, D. H., Kuhn, M. A., Gagné, M., Jensen, E. L. N., & Miller, N. A. 2008, MNRAS, 386, 1855
Corcoran, M. F., Liburd, J., Morris, D., et al. 2017, ApJ, 838, 45
Corcoran, M. F., Nichols, J. S., Pablo, H., et al. 2015, ApJ, 809, 132
Cox, A. N. 2000, Allen's Astrophysical Quantities (4th ed.; New York: AIP)
Dickey, J. M., & Lockman, F. J. 1990, ARA&A, 28, 215
Doyle, T. F., Petit, V., Cohen, D., & Leutenegger, M. 2017, in IAU Symp. 329, The Lives and Death-Throes of Massive Stars, ed. J. J. Eldridge et al. (Cambridge: Cambridge Univ. Press), 395
Drechsel, H., Lorenz, R., & Mayer, P. 1989, A&A, 221, 49
Fruscione, A., McDowell, J. C., Allen, G. E., et al. 2006, Proc. SPIE, 6270, 62701V
Garmire, G. P., Ricker, G. R., Bautz, M. W., et al. 1992, AIAA, Space Programs and Technologies Conference (Reston, VA: AIAA)
Gayley, K. G. 2009, ApJ, 703, 89
Gosset, E., & Nazé, Y. 2016, A&A, 590, A113
Han, W., Kim, C.-H., Lee, W.-B., & Koch, R. H. 2002, AJ, 123, 2724
Harvig, V. 1990, PTarO, 53, 115
Holmgren, D. E., Hill, G., & Fisher, W. 1990, A&A, 236, 409
Huenemoerder, D. P., Oskinova, L. M., Ignace, R., et al. 2012, ApJL, 756, L34
Kim, C.-H., Nha, I.-S., & Kreiner, J. M. 2005, AJ, 129, 990
Lomax, J. R., Nazé, Y., Hoffman, J. L., et al. 2015, A&A, 573, A43
Mayer, P., & Wolf, M. 1986, IBVS, 2886, 1
Muijres, L. E., Vink, J. S., de Koter, A., Müller, P. E., & Langer, N. 2012, A&A, 537, A37
Nazé, Y. 2009, A&A, 506, 1055
Nazé, Y., Broos, P. S., Oskinova, L., et al. 2011, ApJS, 194, 7
Nazé, Y., Petit, V., Rinbrand, M., et al. 2014, ApJS, 215, 10
Nichols, J., Huenemoerder, D. P., Corcoran, M. F., et al. 2015, ApJ, 809, 133
Oskinova, L. M. 2016, AdSpR, 58, 739
Oskinova, L. M., Todt, H., Ignace, R., et al. 2011, MNRAS, 416, 1456
Owocki, S. P., Sundqvist, J. O., Cohen, D. H., & Gayley, K. G. 2013, MNRAS, 429, 3379
Pablo, H., Richardson, N. D., Moffat, A. F. J., et al. 2015, ApJ, 809, 134
Pachoulakis, I., Pfeiffer, R. J., Kock, R. H., & Stickland, D. J. 1996, Obs, 116, 89
Petit, V., Owocki, S. P., Wade, G. A., et al. 2013, MNRAS, 429, 398
Pillitteri, I., Wolk, S. J., Reale, F., & Oskinova, L. 2017, arXiv:1703.04686
Pittard, J. M., & Parkin, E. R. 2010, MNRAS, 403, 1657
Prilutskii, O. F., & Usov, V. V. 1976, SvA, 20, 2
Prinja, R. K. 1989, MNRAS, 241, 721
Rauw, G., Blomme, R., Nazé, Y., et al. 2016, A&A, 589, A121
Rauw, G., & Nazé, Y. 2016, AdSpR, 58, 761
Richardson, N. D., Moffat, A. F. J., Gull, T. R., et al. 2015, ApJ, 808, 88
Sana, H. 2017, arXiv:1703.01608
Shenar, T., Oskinova, L., Hamann, W.-R., et al. 2015, ApJ, 809, 135
Shultz, M., Wade, G. A., Alecian, E. & BinaMIcS Collaboration 2015, MNRAS, 454, L1
Stevens, I. R., Blondin, J. M., & Pollock, A. M. T. 1992, ApJ, 386, 265
Usov, V. V. 1992, ApJ, 389, 635
Vink, J. S., de Koter, A., & Lamers, H. J. G. L. M. 2000, A&A, 362, 295
Yakut, K., Aerts, C., & Morel, T. 2007, A&A, 467, 647